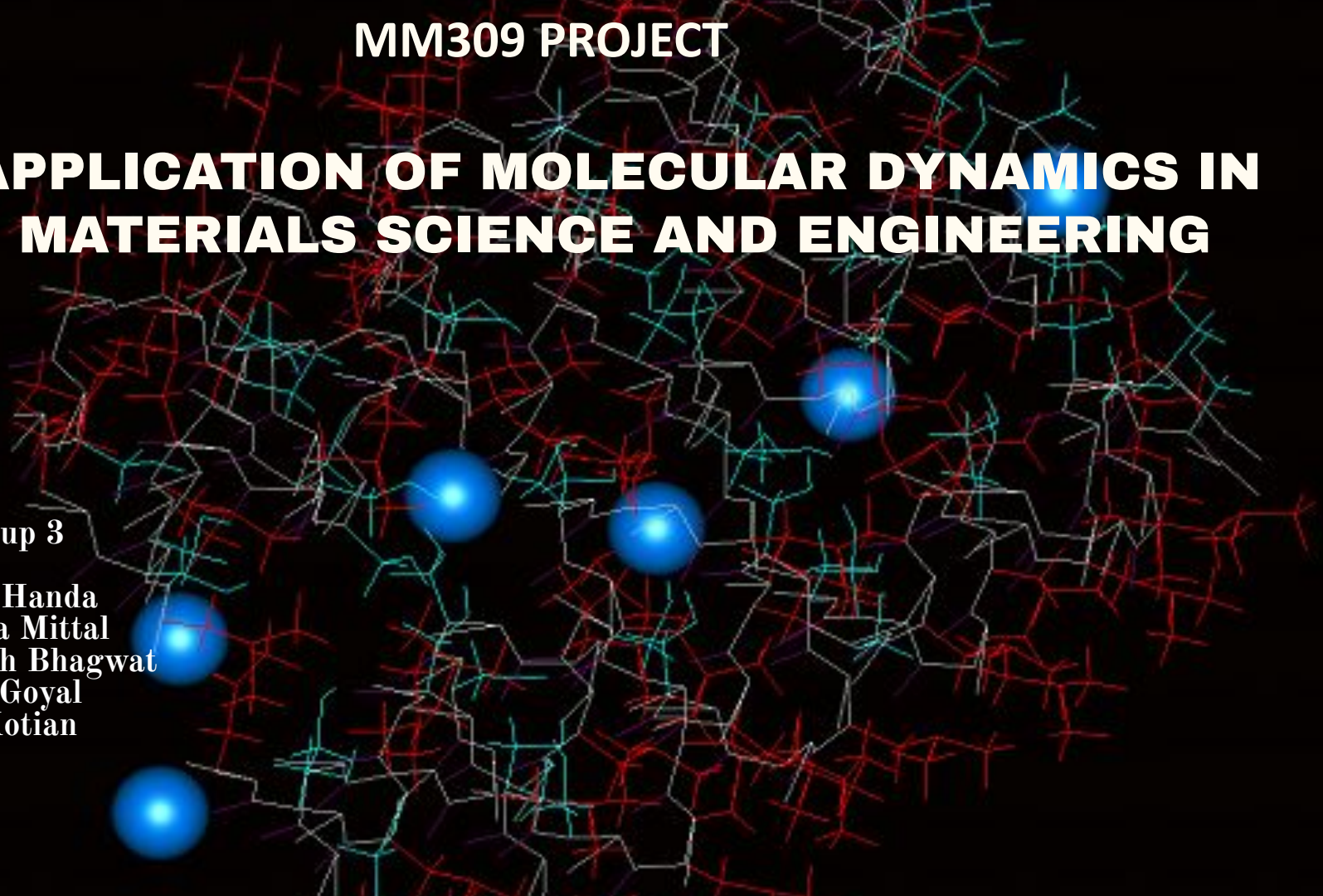**MM309 PROJECT**

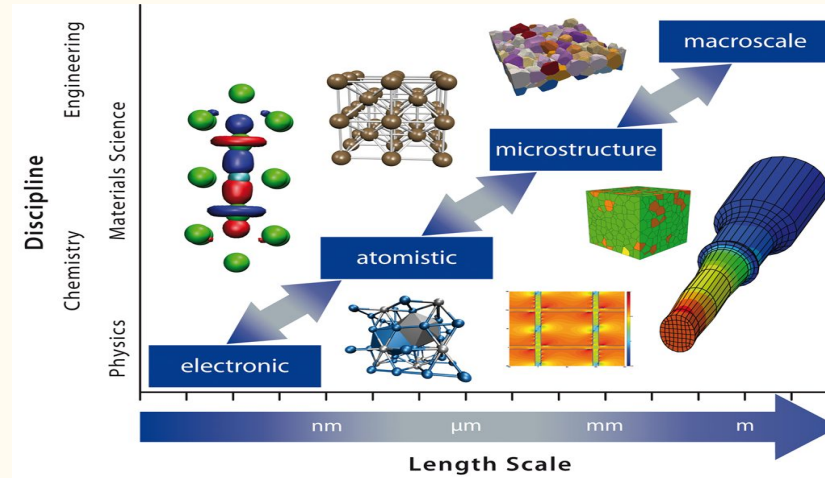# APPLICATION OF MOLECULAR DYNAMICS IN MATERIALS SCIENCE AND ENGINEERING

By Group 3

Aditya Handa
Akshita Mittal
Anirudh Bhagwat
Daksh Goyal
Sejal Kotian

# Introduction to Molecular Dynamics



Molecular dynamics (MD) is a computer simulation method for analyzing the physical movements of atoms and molecules. For a fixed amount of time, the atoms and molecules are allowed to interact, providing insight into the system's dynamic "evolution."

# Molecular Dynamics Simulation

Molecular dynamics simulation is a simulated computer method, through the equations for a group of interactive atomic motion equations, investigates its evolutionary behavior over time. In a molecular dynamics simulation, the movement of atoms follows the classical mechanics required by Newton's laws. In a system formed by N atoms, with other atoms interacting with each other, the force received by each atom as:

$$m_j \frac{d^2\mathbf{r}_j}{dt^2} = \mathbf{F}_j, \qquad \mathbf{F}_j = -\frac{\partial V}{\partial \mathbf{r}_j}, \quad j = 1, 2, \cdots, N$$

The above equation shows that molecular dynamics is a deterministic method, that is, given an initial position and initial velocity, the whole system along with the time evolution locus can be completely determined theoretically.

# Molecular Dynamics Numerical Method

The molecular dynamics numerical method is based on the familiar Newton motion equation. Given an initial speed and displacement to the atoms whose quality is m, the force every atom which is embedded in the atomic method (EAM) received could be calculated. Then a new speed and displacement will be obtained based on a dynamic equation.

Molecular dynamics involves different algorithms, commonly used as the following:

**1)Verlet Algorithm**
**2)Gear Algorithm**

# Verlet Algorithm

$$x_i(t + \Delta t) = x_i(t) + v_i(t)(\Delta t) + \frac{1}{2!}a_i(t)(\Delta t)^2$$

$$v_i(t + \Delta t) = v_i(t) + \frac{\Delta t}{2}\left(\frac{F(t) + F(t + \Delta t)}{m}\right)$$

General Procedure:
1) Find the position
2) Find Force
3) Find the Velocity and repeat

This will generate trajectories of position and velocity computed at t=0; t=delta t, t= 2*delta t, t=3*delta and so on.

# Gear Predictor-Corrector Algorithm

$$\begin{cases} \vec{r}_i^p(t+\delta t) = \vec{r}_i(t) + \vec{v}_i(t)\delta t + \frac{1}{2}\vec{a}_i(t)\delta t^2 + \frac{1}{6}\vec{b}_i(t)\delta t^3 \\[2mm] \vec{v}_i^p(t+\delta t) = \vec{v}_i(t) + \vec{a}_i(t)\delta t + \frac{1}{2}\vec{b}_i(t)\delta t^2 \\[2mm] \vec{a}_i^p(t+\delta t) = \vec{a}_i(t) + \vec{b}_i(t)\delta t \\[2mm] \vec{b}_i^p(t+\delta t) = \vec{b}_i(t) \end{cases}$$

**Predictor stage**

The gear predictor-corrector algorithm predicts the next set of positions and accelerations and then compares the accelerations and predictions to commute a correction for each step. Each step is thus refined literately.

The predictor uses Taylor Series up to higher order(qth order) derivatives at each time step. Coefficients are tabulated for the qth-order predictor.

# Applications of Molecular Dynamics in Materials Science Engineering

- *Applications in the Nanocrystalline Cutting process.*

- *Applications in Carbon Nanotubes*

- *Application in the Solidification and Melting*

- *Application in the Mechanical Deformation of Nanocrystalline materials*

- *Applications in Nanoindentation Measurement*

# MOLECULAR DYNAMICS SIMULATION OF THE NANOMETRIC CUTTING PROCESS

Q. X. PEI and C. LU Institute of High Performance Computing 1 Science Park Road, Singapore 117528

F. Z. FANG and H. WU Singapore Institute of Manufacturing Technology 71 Nanyang Drive, Singapore 638075

# Introduction

Nanoscale machining involves changes in only a few atomic layers at the surface. Molecular dynamics (MD) simulation can play a significant role in addressing a number of machining problems at the atomic scale.

Nanometric machining is a tool-based material removal process that generates ultraprecision surfaces at a nanometer scale. It is used in component manufacturing in electronics industry, aerospace industry, etc.

In the given paper, Instead of the widely used Morse potential, Embedded Atom Method (EAM) potential is used for the study.

Morse potential takes in consideration of only diatomic interaction energy between atoms.

$$V(r) = D_e \left(1 - e^{-a(r-r_e)}\right)^2$$

Embedded Atom Method (EAM) on the other hand evaluates interaction energy as a function of a sum of functions of the separation between an atom and its neighbors.

$$E_i = F_\alpha \left( \sum_{j \neq i} \rho_\beta(r_{ij}) \right) + \frac{1}{2} \sum_{j \neq i} \phi_{\alpha\beta}(r_{ij}),$$

In the paper, copper metal is machined by a diamond tip cutting tool. EAM is better model as it gives realistic energy approximation in a metallic lattice of Cu (atoms interact not with just nearest neighbours but a lot of atoms).

# Simulation Model

- The workpiece consists of 10500 atoms with the dimensions of 35a × 15a × 5a, where a is the lattice constant of copper (3.62 Å).
- Rake angle is taken as 45°, 0°, and −45°. Tool speed is varied from 10m/s to 100 m/s.
- Boundary condition: bottom boundary and left most boundary are fixed.
- Periodic boundary conditions are maintained along the z direction
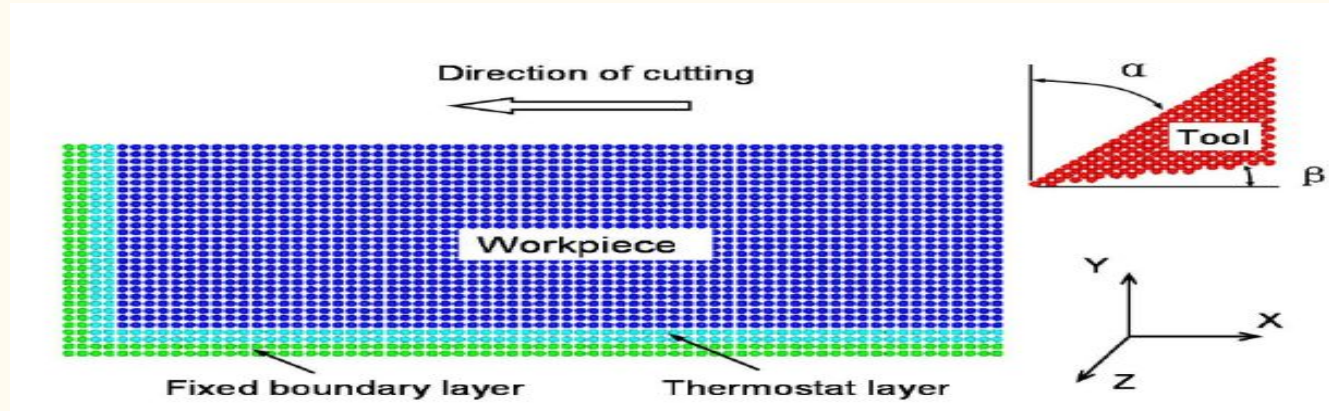
# Simulation Results and Discussion

As seen in image, the tool chips the desired surface but different distortions in nearby region are created in different cases.

Chipping is easiest in case of positive rake angle ($+45°$), as applied force results in high shear strain which is desired.

Chipping gets more and more difficult as angle reduces and ultimately becomes -ve. Now a lot of applied force is wasted in tensile compression of atoms.
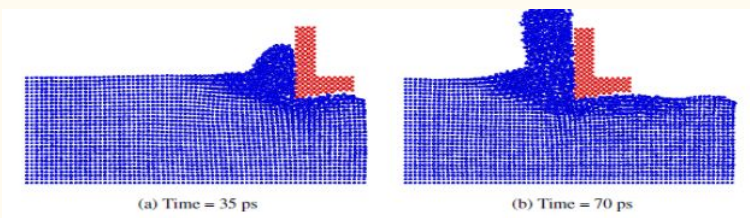


(a) Time = 35 ps       (b) Time = 70 ps

Fig. 2. The nanometric cutting process with the tool rake angle 0° and the cutting speed of 100 m/s.

(a) Time = 35 ps       (b) Time = 70 ps

Fig. 3. The nanometric cutting process with the tool rake angle 45° and the cutting speed of 100 m/s.

(a) Time = 35 ps       (b) Time = 70 ps
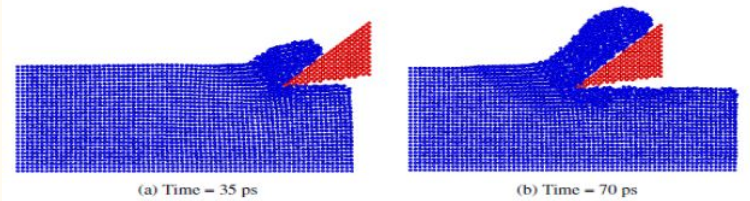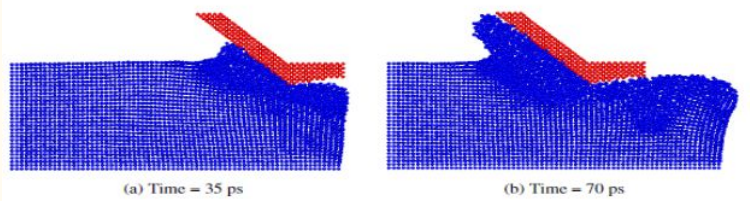
Fig. 4. The nanometric cutting process with the tool rake angle −45° and the cutting speed of 100 m/s.

Table 1. The cutting force for different tool rake angles.

| Tool rake angle (degree) | Horizontal force $F_x$ (nN) | Vertical force $F_y$ (nN) |
|---|---|---|
| 45 | 21.7 | 6.1 |
| 0 | 34.7 | 19.8 |
| −45 | 39.8 | 59.7 |

# Conclusion

- The tool rake angle has a big effect on the material removal and chip formation. As the rake angle decreases from $45°$ to $−45°$, the chip deforms from more shear deformation to more compression deformation, and the machined surface becomes rougher.

- As the rake angle decreases from $45°$ to $−45°$, both the horizontal and vertical cutting forces increase significantly.

- The low cutting speed favors a smooth surface, while the high cutting speed results in a rough surface.

# Molecular dynamics simulations of the elastic properties of polymer/carbon nanotube composites

—

Akshita Mittal
200005005

# Molecular dynamics simulations of the elastic properties of polymer/carbon nanotube composites

- CNT's are promising additives to Polymeric Materials

- Potential for enhancement of mechanical, structural and electronic properties

- Improvements are not guaranteed, and results depend on the polymer chosen, quantity and quality of the CNT
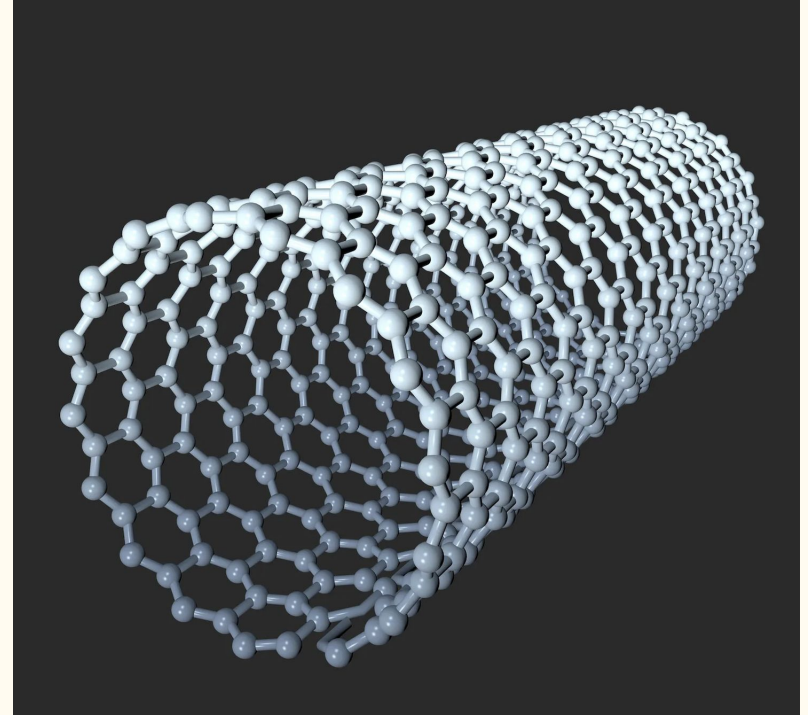
## Molecular dynamics simulations of the elastic properties of polymer/carbon nanotube composites

Yue Han, James Elliott *

*Department of Materials Science and Metallurgy, University of Cambridge, Pembroke Street, Cambridge CB2 3QZ, UK*

Received 21 November 2005; received in revised form 14 June 2006; accepted 20 June 2006

**Abstract**

Carbon nanotubes (CNTs) are promising additives to polymeric materials due to the potential for their enhancement of the structural, mechanical and electronic properties of the resulting composite. However, improvements in properties are by no means guaranteed, and the results are often sensitive to the particular polymer chosen, in addition to the quantity and quality of CNTs used in the composite. In this paper, we present classical molecular dynamics (MD) simulations of model polymer/CNT composites constructed by embedding a single wall (10,10) CNT into two different amorphous polymer matrices: poly(methyl methacrylate) (PMMA) and poly{(*m*-phenylene-vinylene)-*co*-[(2,5-dioctoxy-*p*-phenylene) vinylene]} (PmPV), respectively, with different volume fractions. A constant-strain energy min-imization method was then applied to calculate the axial and transverse elastic moduli of the composite system. The simulation results support the idea that it is possible to use CNTs to mechanically reinforce an appropriate polymer matrix, especially in the longitudinal direction of the nanotube. In addition, the results show that detailed interfacial ordering effects cannot be ignored when interactions between the nanotube and polymer matrix are strong. The comparison of the simulation results with the macroscopic rule-of-mixtures for composite systems showed that for strong interfacial interactions, there can be large deviations of the results from the rule-of-mixtures.

In this paper, Classical molecular dynamics (MD) simulations of model polymer/CNT composites are done:

We embed a **single wall (10,10) CNT** into two different amorphous polymer matrices:

- poly(methyl methacrylate) **(PMMA)**
- poly{(m-phenylene-vinylene)-co-[(2,5-dioctoxy-p-phenylene) vinylene]} **(PmPV)**

with **different volume fractions.**

# Motivation

To apply a *constant-strain energy minimization* method to calculate the axial and transverse elastic moduli of the composite system.

# Background on CNT's in Polymers

- The performance of a fibre-reinforced composite depends critically on the interfacial characteristics between the fibres and the matrix material.

- Strong fibre–matrix interfaces - **high composite stiffness and strength**, **but low composite toughness** and vice versa.

- With nanotube-based composites:
  **Speculation**: is the strength of the interface between CNTs and polymer matrices significant at all?
  This is where
  **MOLECULAR DYNAMICS** **comes into picture**
  **Since experimental methods for measurements are rather difficult.**

# Background on CNT's in Polymers

**1** The extent to which mechanical reinforcement can be achieved depends on
- **uniformity of dispersion**
- **degree of alignment of CNTs**
- **the strength of polymer–CNT interfacial bonding**
- **Total nanotube Surface area**

**2** It is difficult to control and measure many of these properties **experimentally**

**3** For this reason, **computational modelling** has been widely applied to study polymer/CNT composites.
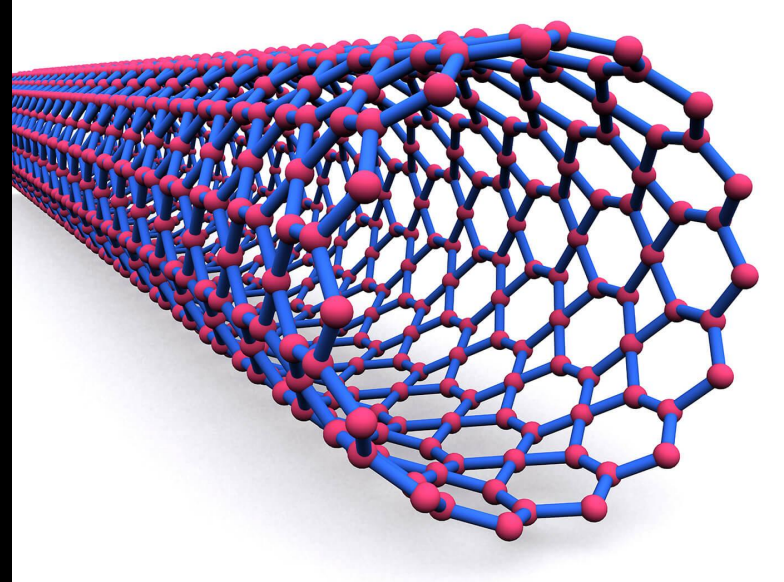
# What are we trying to determine using the simulations?

In general,

- **Semicrystalline thermoplastic polymers** - large strains
- **Amorphous materials** - only small elastic strain before either fracture or yielding takes place.

**UTS or yield stress** - governed by the **presence of defects**,
For calculating UTS or Yield Stress, bulk properties of the material → more pertinent than the local atomic structure.

Hence, it is **computationally very difficult** to calculate the **strength of pure polymer systems and composite systems** undergoing **large** plastic deformation using the MD Method.

Due to this reason, the current study focuses on the calculation of **low strain elastic moduli only**

**Motivation**- elucidation of the effect of **interfacial interaction energy between CNTs and polymer matrix.**

# Building Molecular Model of the Polymer Matrix
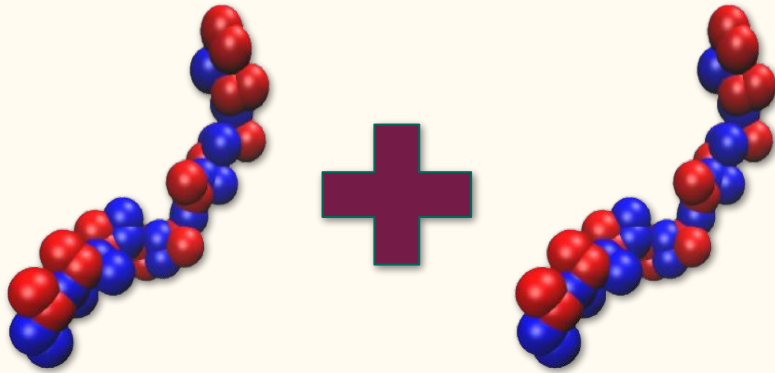


Two chains of PMMA (80% syndiotactic) - each with 50 repeat units

Built in a Periodic Box

With Initial density = 0.1g/cm3

Using DREIDING Force Field Parameters

# Building Molecular Model of the Polymer Matrix

- The model was put into an **NPT ensemble simulation** **Pressure = 10 atm Temperature = 500 K** for **1 ns (the simulation time step was 1 fs)**.

- The purpose of this step was to slowly compress the structure to generate initial amorphous matrix with the correct density and low residual stresses.

- Attempts to further increase pressure using the **DREIDING force field** failed to generate a density close to the experimental value.

- The **COMPASS force field** was then applied under the same conditions for another **500 ps**.

- Simulation temperature was set to **298 K**, and **pressure of 1 atm** for another **500 ps**.

- The density of the final matrix was **1.15 g/cm3**, which is very close to the experimental value of **1.19 g/cm3.**

- After this, a **constant-strain minimization** was carried out with the strain being varied from **0% to 2%** in discrete steps.

# Calculating the elastic moduli

**Constant-strain energy minimization method** was applied to calculate the elastic moduli of the polymer/CNT composite system.

Small strains were applied to a periodic structure at an energy minimum.

*Application of strain* : accomplished by uniformly expanding the dimensions of the simulation cell in the direction of the deformation and re-scaling the new coordinates of the atoms to fit within the new dimensions.

The structure was then re-minimized keeping the lattice parameters fixed, and the resultant stress in the minimized structure was measured.

This was repeated for a series of strains. The variation of the measured stress as a function of applied strain was used to derive the stiffness matrix.

# Computational Results

A (10,10) SWNT (Single Walled Nano-Tube) was placed in the centre of a periodic simulation cell. PmPV molecules with different number of repeat units were then placed randomly around the tube in non-overlapping positions. A similar process was followed for PMMA Matrix.

A similar equilibration process as used for generating the matrix model was applied to generate the composite model.

**The interaction energy** between
- **PmPV matrix and CNT** was calculated to be about (-360 ± 30) kcal/ mol
- **PMMA matrix and CNT** was calculated to be about (-243 ± 30) kcal/mol
  by the present simulation.

The magnitude of the error represents the spread of values of the interaction energy averaged over 10 independently constructed configurations, with the negative sign indicating attraction between the matrix material and the nanotube.
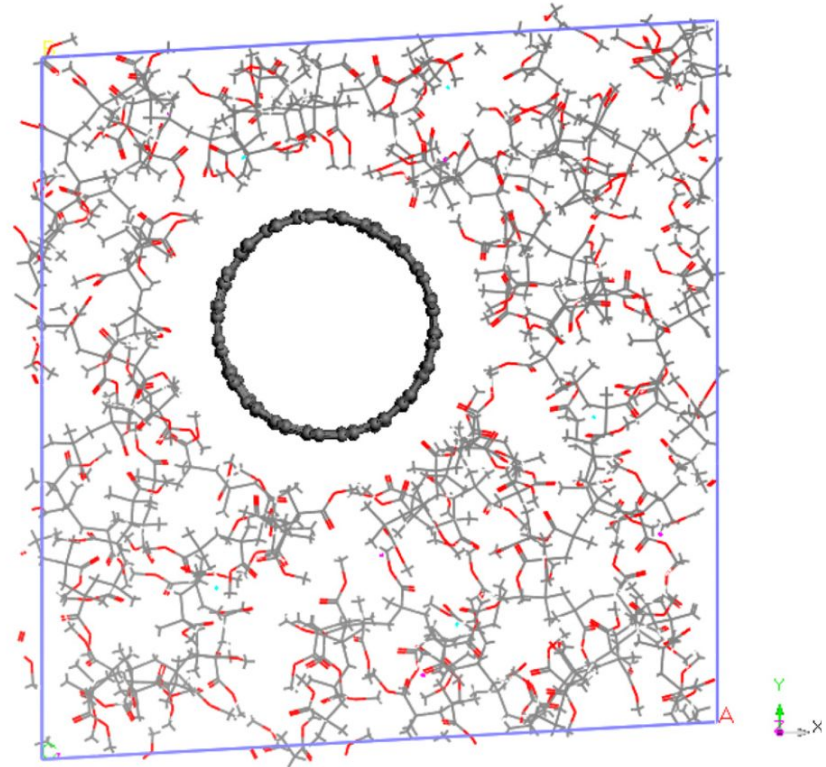
# Computational Results



*Snapshot of a MD simulation model of (10,10) SWNT and PmPV molecule in vacuo. Only the backbone of the PmPV molecule is visible in the graph. The SWNT is shown here as small dots.*
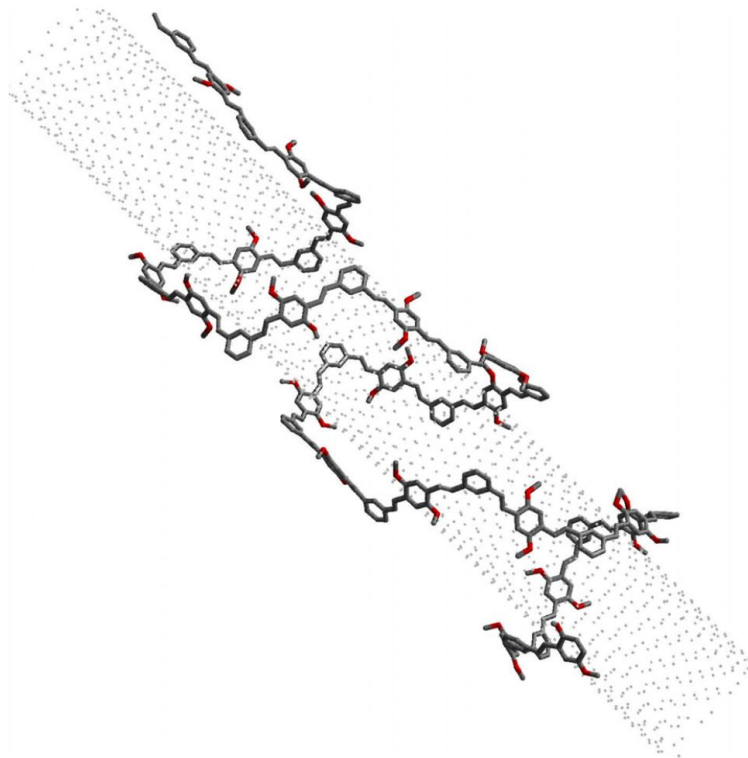
# Computational Results

Snapshot of a MD simulation cell of the PMMA/CNT composite

# Analysis of Results

Following equilibration, the amorphous models of PmPV/CNT composites with different CNT volume fractions were then subjected to **constant-strain minimization** for the calculation of mechanical properties.

We plotted the **stress–strain curves** for **transverse and axial loading conditions** for different volume fractions of CNT in PmPV and PMMA Matrix composites.
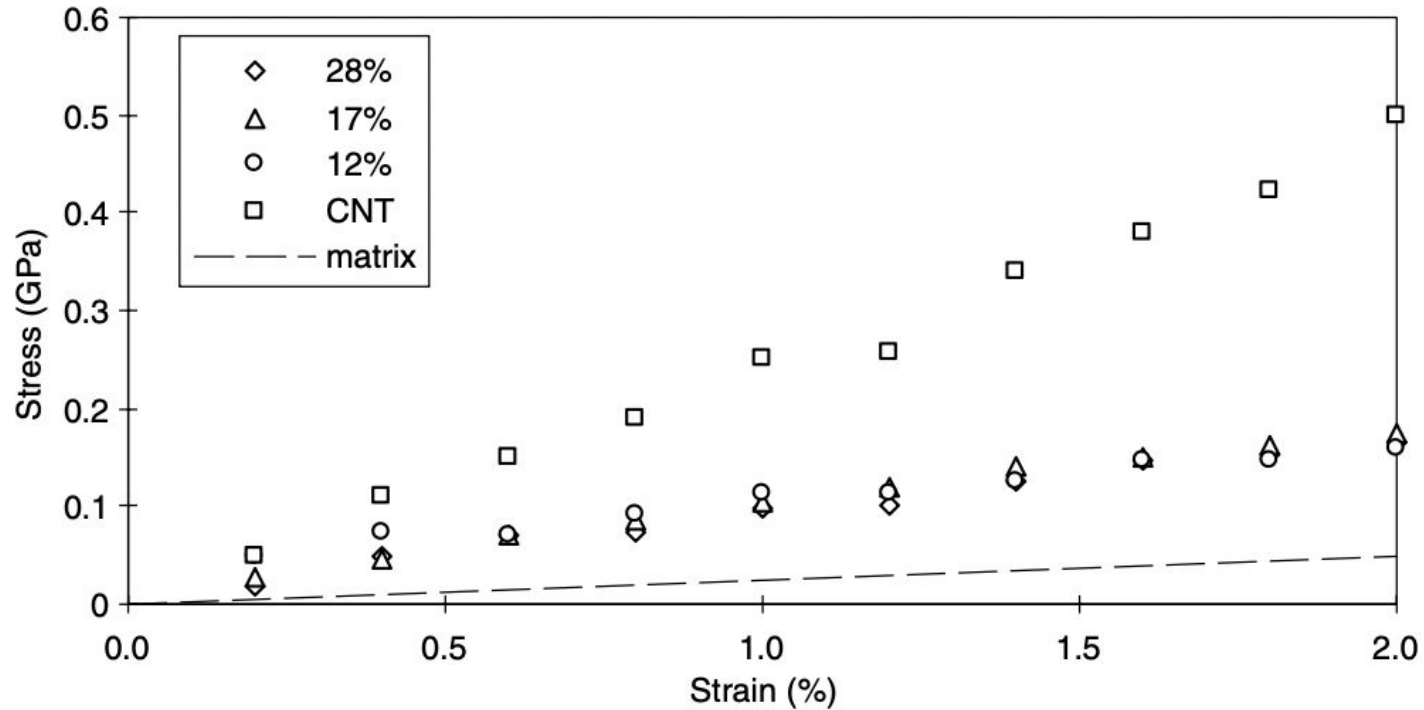
*Stress–strain curves in the **transverse direction** for **PmPV/CNT** composites with different CNT volume fractions*
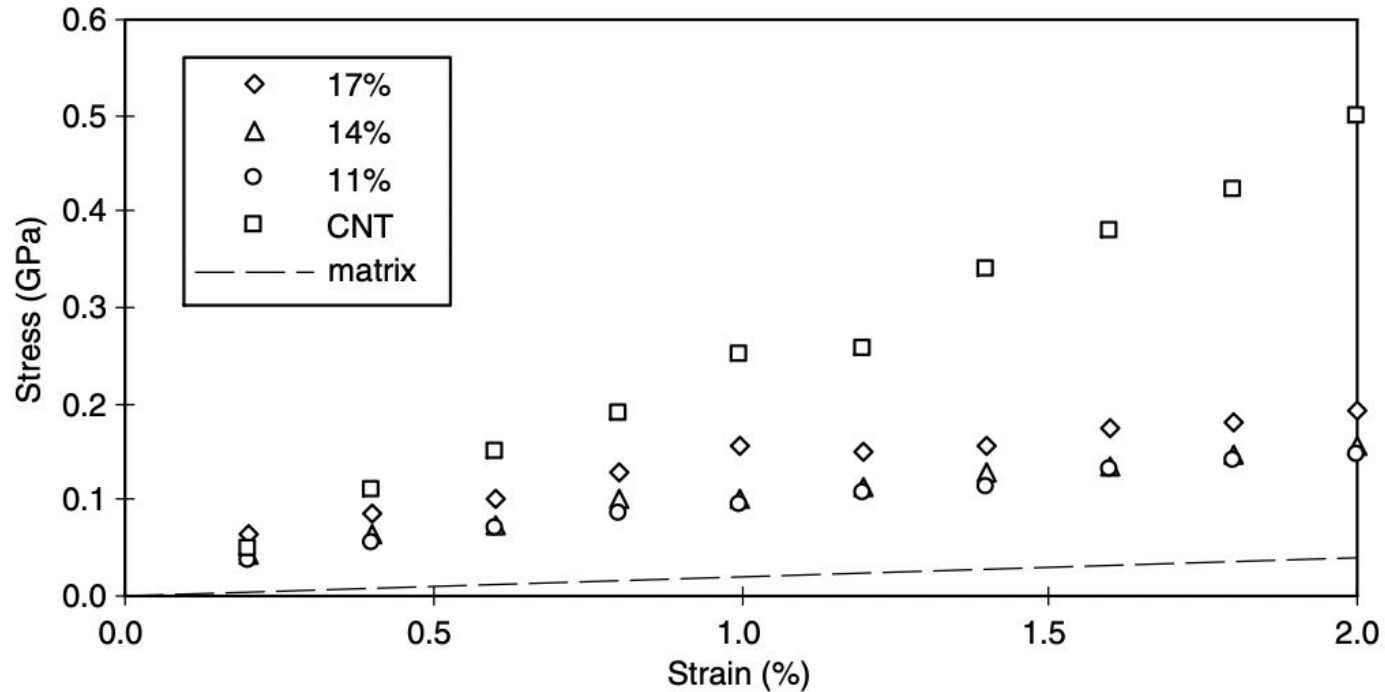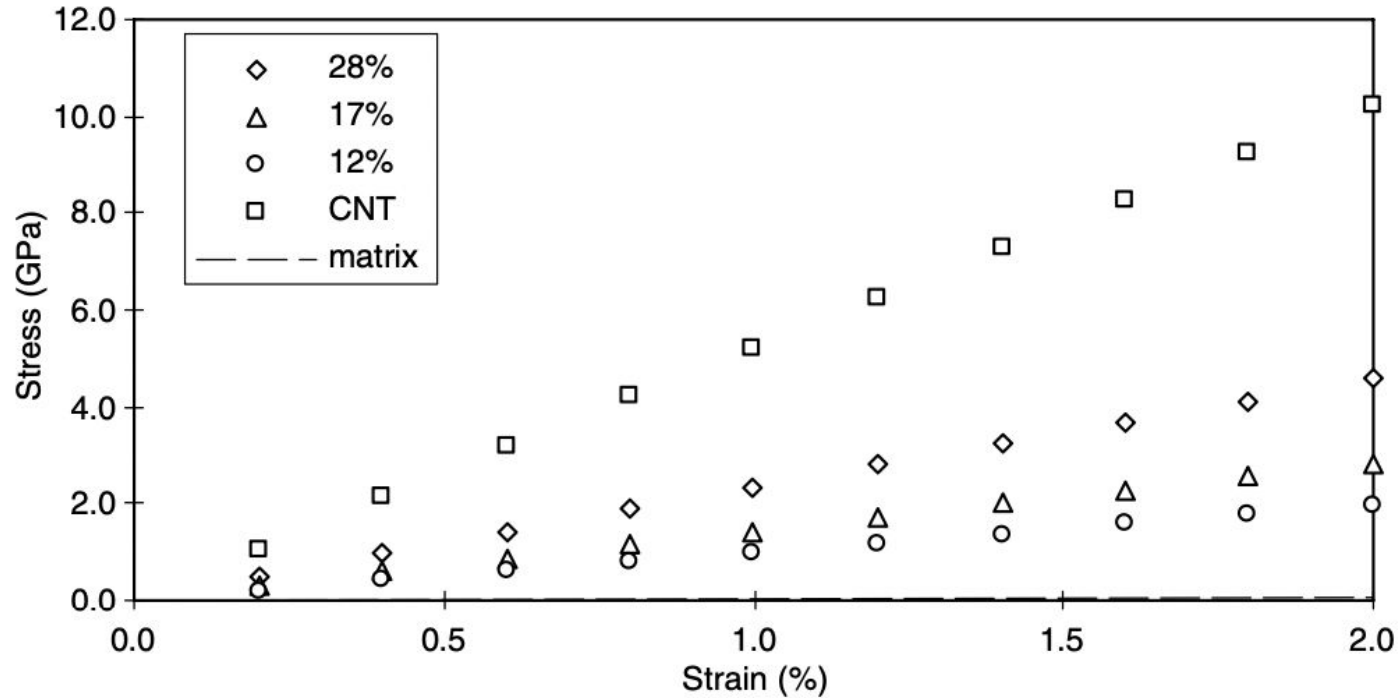
*Stress–strain curves in the **longitudinal direction** for **PmPV/CNT** composites with different CNT volume fractions*
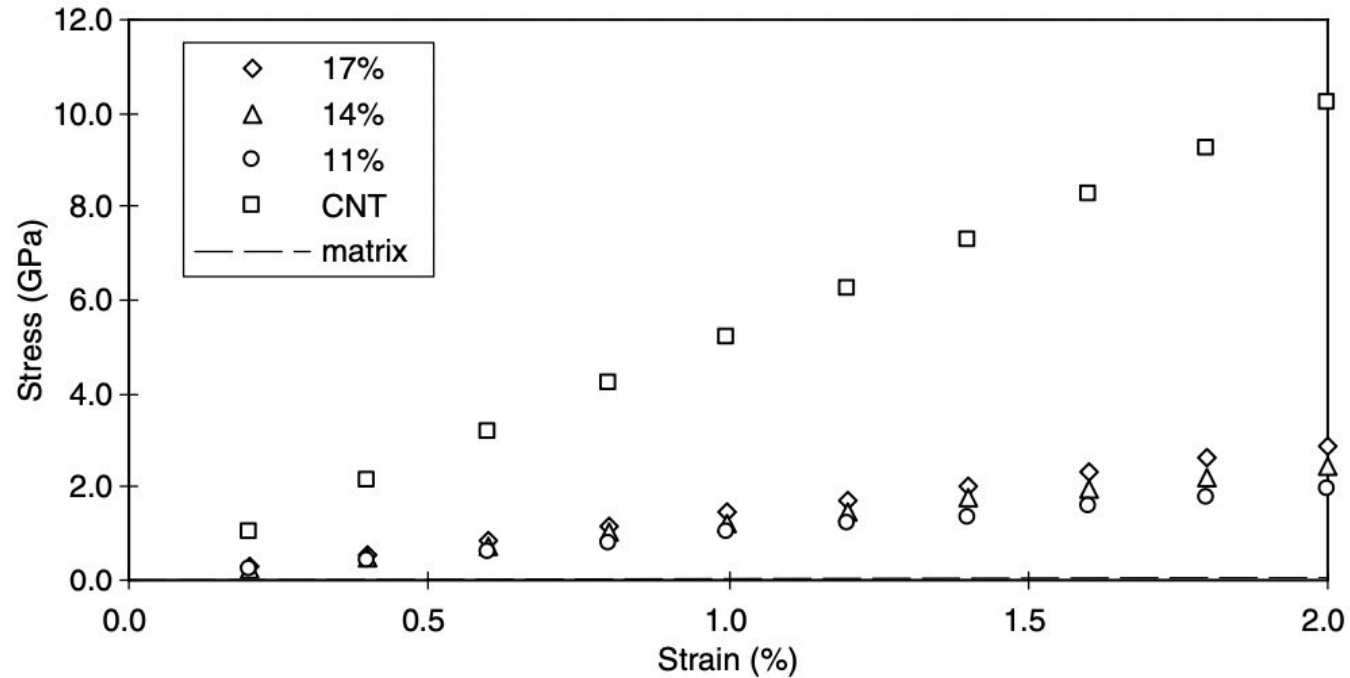
*Stress–strain curves in the **transverse direction** for **PMMA/CNT** composites with different CNT volume fractions*

*Stress–strain curves in the **longitudinal direction** for **PMMA/CNT** composites with different CNT volume fractions*

# Analysis of the graphs

**PmPV/CNT Composite**

From the stress–strain curves for different directions, it is seen that subjected to transverse loading condition, there is **no strong reinforcement of the matrix**.

In the **longitudinal direction**, the slope of the stress–strain curve (i.e. the Young's modulus) clearly increases with the increasing of CNT volume fraction, since the CNTs carried most of the load in this direction.

**PMMA/CNT Composite**

Again, it can be seen that the reinforcement behaviour in the **longitudinal loading direction** is **much stronger** than that in the transverse direction.

*The difference in longitudinal and transverse behaviour,, illustrate the anisotropy of the composite material.*

# LAMMPS INPUT SCRIPT for NPT ENSEMBLE

# LAMMPS input for NPT simulation

variable dt equal 0.001

variable lp equal 5.34

variable T equal 35

variable P equal 0

# some parameters/instructions

dimension 3

units metal

boundary p p p

atom_style atomic

timestep ${dt}

dump 1 all atom 5000 config.dump

# LAMMPS INPUT SCRIPT for NPT ENSEMBLE

# initial position

lattice fcc ${lp} orient x 1 0 0 orient y 0 1 0 orient z 0 0 1

region mybox block 0 5 0 5 0 5

create_box 1 mybox

create_atoms 1 region mybox

# define the potential and mass

mass 1 39.948

pair_style lj/smooth 7.5 8.5

pair_coeff 1 1 0.01042 3.4

# perform energy and force minimization

minimize 1e-20 1e-20 10000 10000

```
velocity all create $T 12345 mom yes rot yes dist gaussian

# specify NPT run

fix fNPT all npt temp $T $T 0.1 iso $P $P 1.0

# output format in log file

thermo_style custom step temp press vol ke pe etotal

thermo 20

# writing thermodynamic data to a file npt.dat

variable vtm equal temp

variable vpr equal press

variable vvl equal vol

variable vke equal ke

variable vpe equal pe
```

```
fix fT all ave/time 5 100 500 v_vtm v_vpr v_vvl v_vke v_vpe v_vet file npt.dat

# run simulation

run 100000

# simulation over for initial temperature

unfix fNPT

# increase temperature

variable 2T equal 2*$T

fix fNPT all npt temp ${2T} ${2T} 0.1 iso $P $P 1.0

run 50000

unfix fNPT

# increase temperature
```

```
variable 3T equal 3*$T

fix fNPT all npt temp ${3T} ${3T} 0.1 iso $P $P 1.0

run 50000

unfix fNPT

undump d1
```

# Conclusion

- Molecular dynamics (MD) and energy minimization simulation methods were employed to investigate the elastic moduli of the polymer/CNT composite systems.
- Both PMMA and PmPV matrices were studied and compared.
- The simulation results suggested the possibility of using CNTs to mechanically reinforce both of these two polymer matrices (by increasing the low strain elastic modulus), especially in the tube longitudinal direction.
- For a fixed tensile load, the CNTs should be aligned parallel with the loading direction to produce the largest tensile modulus. In addition, the results show that interfacial effects cannot be ignored when interactions between the nanotube and polymer matrix are strong.

# Reference Research Paper

Molecular dynamics simulations of the elastic properties of polymer/carbon nanotube composites

*Yue Han, James Elliott*

*Department of Materials Science and Metallurgy, University of Cambridge, Pembroke Street, Cambridge CB2 3QZ, UK*

# Molecular dynamics simulation of melting, solidification and remelting processes of aluminum

—

Ref:
https://www.researchgate.net/publication/260337336_Molecular_dynamics_simulation_of_melting_solidification_and_remelting_processes_of_aluminum

# INTRODUCTION

- MD can be used to study the crystallization and glass formation processes of metals during rapid solidification.
- The MD simulation results offer insight into the local structural features and the accompanying thermal dynamics qualities under strong quenching settings.
- The cooling rates employed here are significantly higher than laboratory quick quenching rates.

# INTRODUCTION

- Sutton-Chen many body potential has been used in a molecular dynamics simulation study to look into the solidification and remelting of aluminum.
- Sutton-Chen Potential is governed by the following equations

$$V = \sum_i \left[ \sum_{j>i} \left( \frac{\epsilon_{ij}\sigma_{ij}}{r_{ij}} \right)^{n_{ij}} - \epsilon_i c_i \sqrt{\rho_i} \right]$$

$$\rho_i = \sum_{j \neq i} \left( \frac{\sigma_{ij}}{r_{ij}} \right)^{m_{ij}}$$

- Different number of atoms were considered (108-2048) to find adequate size of the system.
- The simulation was carried out on different cooling and heating rates.

# SIMULATION - Parameters

- All the simulations were ran in 3-Dimensions
- Canonical Ensemble (NVT) with time step of 0.1fs was used.
- Periodic Boundary Conditions were used.
- Motion Equations were solved numerical using Verlet Algorithm.
- Simulation was ran on different systems of sizes 108, 256, 500, 864, 1372 and 2048 atoms.
- The following numbers were chosen as to fill the complete cell for Aluminium(fcc).
- Various Heating and Cooling rates were applied. ($10^{12}$K/sec - $10^{14}$K/sec).
- Temperature Cycle
  - Melting: 300K - 1300K equilibration at 300K
  - Solidification: 1300K - 300K
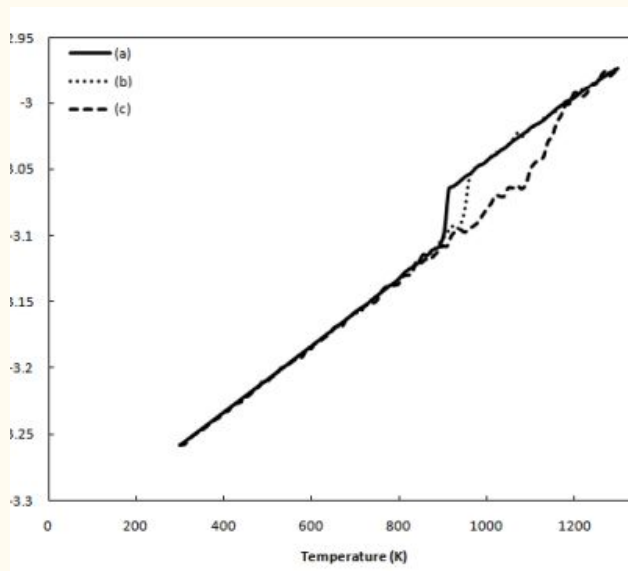
# Simulation - Results

### For Melting

- Melting Point was lowered upon increasing number of atoms and finally became constant.
- The melting temperature decreases because the system needs a minimum number of atoms to be stable.
- So for further simulations number of atoms were fixed to 500.

| Number of Atoms | Melting Temperature(K) |
|:---:|:---:|
| 108 | 1060 |
| 256 | 970 |
| 500 | 940 |
| 864 | 940 |
| 1732 | 940 |
| 2048 | 940 |

# Simulation - Results

### For Melting

- A sudden increase in Internal Energy was observed around 900K temperature.
- This is due to start of change in structure from crystalline to liquid around 900K.

- While at 1100 K a small fraction of crystalline structure was reserved, full liquid structure was obtained at 1200K.
- When the heating rate increased, the phase transformation temperature shifted to a higher temperature range

# Simulation - Results

For Solidification
- A sharp decrease in Internal Energy was observed on cooling around 460K at rate of 10^12K/sec.
- No crystallization was observed at higher cooling rates.
- The reduction in moving range was observed in MSD data on cooling.
- MSD at lower cooling rates were higher.
- At higher cooling rates metallic glass structure was formed, which is an amorphous-like structure so MSD dosent change significantly.
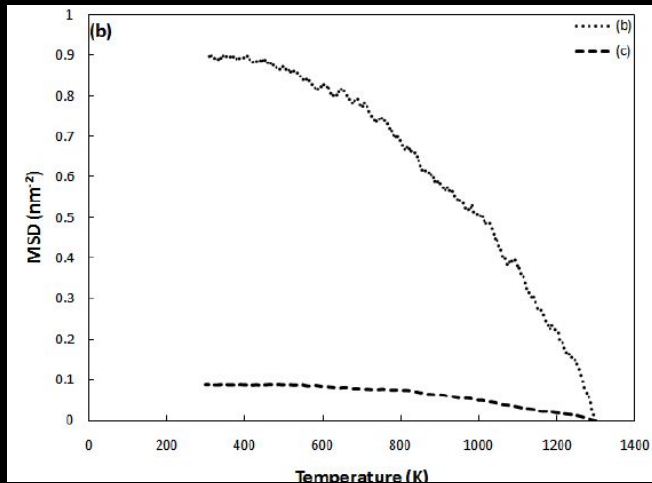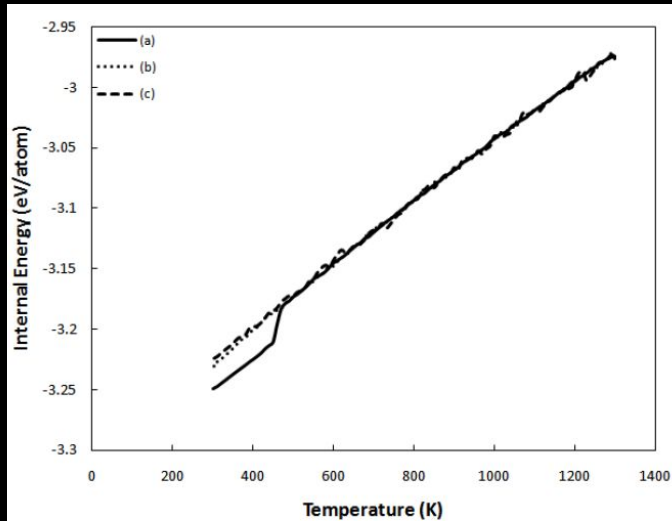
# Conclusion

- The melting temperature of crystalline aluminum depends on the heating rate.

- The melting temperature increased from 896 K to 1135 K with increasing the heating rate from 10^12 K/s to 10^14 K/s.

- The melted aluminum atoms crystallized to FCC structure at 462 K during cooling with a rate of 10^12 K/s. At higher cooling rates, however, amorphous-like structures formed.

# Molecular-Dynamics Study of Mechanical Deformation in Nano-Crystalline Aluminum

—

K. KADAU, T.C. GERMANN, P.S. LOMDAHL, B.L. HOLIAN, D. KADAU, P. ENTEL, M. KRETH, F. WESTERHOFF, and D.E. WOLF

# Introduction

- **The Hall-Petch relation** - gives a quantitative description of an increase in the yield stress of a polycrystalline material as its grain size decreases.

- Inter grain activities such as **rotation, sliding, and growth**.  are dominated at nano-level inverse Hall–Petch relation for Cu, Ni, and Pd for small grain sizes (d 10 nm, where d average grain size) exhibit plasticity.

- Large-scale molecular-dynamics (MD)[10] simulations, performed with the SPaSM code,[11] investigating the tensile loading of nano-crystalline Al.

- The atomic interactions were described by an embedded-atom method(EAM) potential especially designed to model Al.

$$E_i = F_\alpha \left( \sum_{j \neq i} \rho_\beta(r_{ij}) \right) + \frac{1}{2} \sum_{j \neq i} \phi_{\alpha\beta}(r_{ij}),$$

# Computational methods

- Two different methods were used to prepare the nanocrystalline initial sample configuration.
- The first method is a **<u>Voronoi construction,</u>** where grain centers and orientations are randomly chosen, and a subsequent space filling, with the local orientation determined by the closest grain center.
- After annealing at 600 K for 22.5 ps and then equilibrating at 300 K for 22.5 ps, this method gives poly-crystalline structures with **<u>polytope</u>** grains(a geometric object with flat sides).
- The second method is to sinter the sample from spherical nanoparticles with different diameters. As the initial configuration, we took a close-packed arrangement obtained by contact-dynamics simulations consisting of 32 nanoparticles with three different diameters having a ratio of 2:3:4.
- Filling those nanoparticles with a crystal of random orientation and sintering under a pressure of 1 to 2 GPa at a temperature of 600 K for 157.5 ps, followed by a relaxation at zero pressure and T 300 K for 45 ps, results in samples of different density depending on the sinter pressure and the size of the nanoparticles.

- Then relaxation at zero pressure and T 300 K for 45 ps, results in samples of different density depending on the sinter pressure and the size of the nanoparticles.

- It has also been pointed out that in spite of these extremely high strain rates, the Coble-creep equation describing grain boundary diffusion in coarse-grained materials can still be reproduced.

$$\frac{d\epsilon_C}{dt} \equiv \dot{\epsilon}_C = A_C \frac{\delta'}{d^3} \frac{\sigma\Omega}{kT} D_0 e^{-(Q_f+Q_m)/kT} = A_C \frac{\delta'}{d^3} \frac{\sigma\Omega}{kT} D_{GB},$$

- **<u>Inverse Hall–Petch behavior</u>**-The tensile loading simulations show the flow stress decreasing with decreasing grain size.

- Grain boundary **<u>structure and thickness</u>** does not change which is observed by experimental X-ray absorption fine structure techniques and by previous MD studies.

- Samples with larger grain sizes tend to exhibit fracture at smaller strains than do samples with smaller grains.
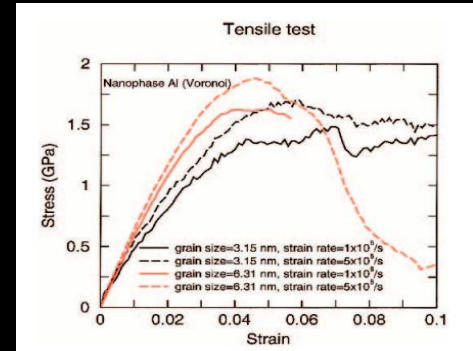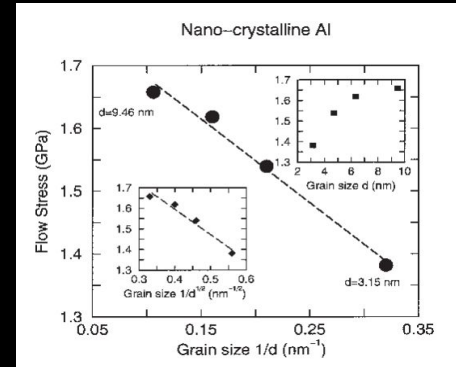
- The deformation mechanism for small grain sizes is related to the **surface-to-volume** ratio of the grains, indicating the dominance of intergrain activity.

- One interesting observation is a "**new mode**" of plasticity for the sintered samples: the more porosity the sample has, the more pronounced is the **growth of pores** and the less pronounced are the grain boundary sliding processes. The growth of pores eventually leads to a fracture starting at pores propagating along grain boundaries.
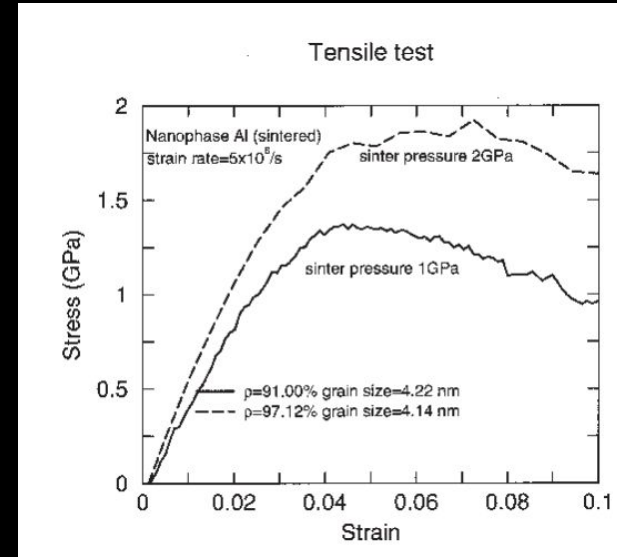


Tensile test

Nanophase Al (sintered)
strain rate=5x10⁶/s
sinter pressure 2GPa
sinter pressure 1GPa
ρ=91.00% grain size=4.22 nm
ρ=97.12% grain size=4.14 nm

**Table I.** Average Grain Size $d$, Density as Compared to the Bulk Value (before Loading), Number of Atoms, and Measured Flow Stresses for Different Strain Rates $\dot{\varepsilon}$ for the Two Different Preparation Methods

| Method | $d$ | Density (Pct Bulk) | Number of Atoms | Flow Stress $\dot{\varepsilon} = 5 \times 10^{-8}$/s | Flow stress $\dot{\varepsilon} = 1 \times 10^{-8}$/s |
|---|---|---|---|---|---|
| Voronoi | 3.15 nm | 97.03 | 55,210 | 1.68 GPa | 1.38 GPa |
| Voronoi | 4.73 nm | 97.69 | 190,785 | — | 1.54 GPa |
| Voronoi | 6.31 nm | 98.15 | 457,422 | 1.87 GPa | 1.62 GPa |
| Voronoi | 9.56 nm | 98.72 | 1,561,466 | — | 1.66 GPa |
| Sinter pressure 2 GPa | 4.14 nm | 97.12 | 129,256 | 1.82 GPa | — |
| Sinter pressure 1 GPa | 3.33 nm | 95.75 | 66,452 | 1.79 GPa | — |
| Sinter pressure 1 GPa | 4.22 nm | 91.00 | 129,256 | 1.37 GPa | — |
| Sinter pressure 1 GPa | 7.25 nm | 83.59 | 600,728 | 0.87 GPa | — |

- Flow stress increases with increasing strain rate.

- In nano-regime sliding processes between the grains dominate the plastic deformation process.

# APPLICATION OF MOLECULAR DYNAMICS IN NANOINDENTATION MEASUREMENT

Sejal Kotian
200005042

The most popular method for determining thin film characteristics like Young's Modulus and hardness in *Nanoindentation*

# Molecular Dynamics Analysis of Temperature Effects on Indentation Measurements

## Molecular dynamics analysis of temperature effects on nanoindentation measurement

Te-Hua Fang [a], Cheng-I Weng [b,*], Jee-Gong Chang [b]

[a] Department of Mechanical Engineering, Southern Taiwan University of Technology, Tainan 710, Taiwan, ROC
[b] Department of Mechanical Engineering, National Cheng Kung University, Tainan 710, Taiwan, ROC

**Abstract**

A three-dimensional molecular dynamics (MD) model is carried out to study the effects of temperature on the atomic-scale nanoindentation process. The model utilizes the Morse potential function to simulate interatomic forces between the sample and tool. The results show that both Young's modulus and hardness become smaller as temperature increases. The results also indicate that elastic recovery is smaller at higher temperatures. The softening behavior is similar to the prior experiment and the estimated elastic moduli are much higher than the prior experiment. The discrepancy may be due to simulations performed on defect-free single crystals. In addition, some defects of vacancies, atomic steps and plastic indent are observed on the surface region.
© 2003 Elsevier Science B.V. All rights reserved.

*Keywords:* Nanoindentation; Molecular dynamics; Young's modulus; Hardness

# Simulation Model

**1** A sample and tool are assumed to consist, respectively, of monocrystalline copper and rigid diamond.

**2** Periodic boundary conditions are used in transverse (x and y) directions and the bottom three layers of atoms of copper are fixed in space.
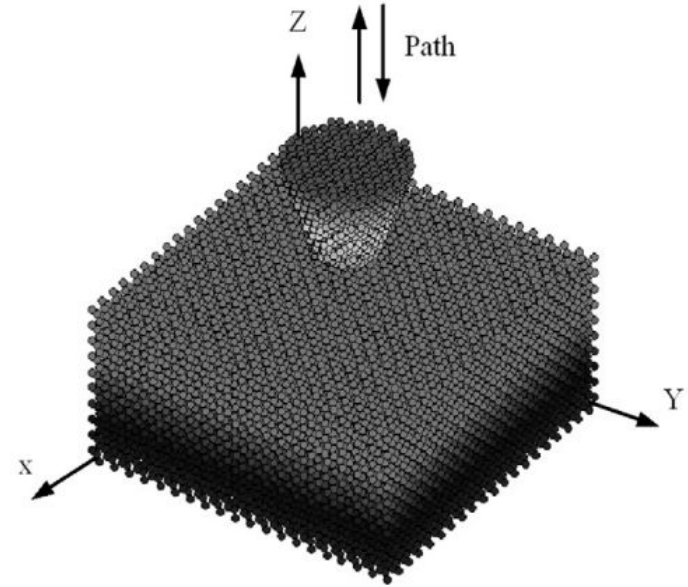


Fig. 1. MD simulation model.

# Simulation Model…Contd

**3** Interatomic forces between the atoms are modeled using the Morse Potential

**4** The force acting on an individual atom is obtained by summing the forces contributed by the surrounding atoms
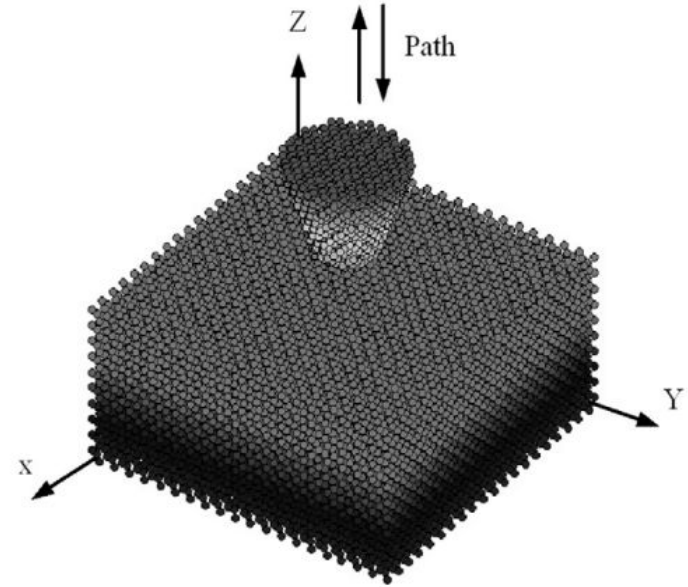


Fig. 1. MD simulation model.

# Morse Potential

## Pair Potential Energy function

for a vibrating diatomic molecule that improves on the simple harmonic oscillator model in that the vibrational levels converge with increasing energy and that at some finite energy the molecule dissociates.

The potential energy, V(R), of a diatomic molecule can be described by the Morse potential:

$$V(R) = D_e \left(1 - e^{-\beta(R - R_e)}\right)^2$$

where $D_e$ is the well depth, R is internuclear distance, $R_e$ is the equilibrium internuclear distance (bond length), and

$$\beta = \pi \nu_e \sqrt{\frac{2\mu}{D_e}}$$

$\nu_e$ is the vibrational constant and $\mu$ is the reduced mass.

# Morse Potential

## Pair Potential Energy function

for a vibrating diatomic molecule that improves on the simple harmonic oscillator model in that the vibrational levels converge with increasing energy and that at some finite energy the molecule dissociates.



Fig. 2. Shape of various Morse type potentials.
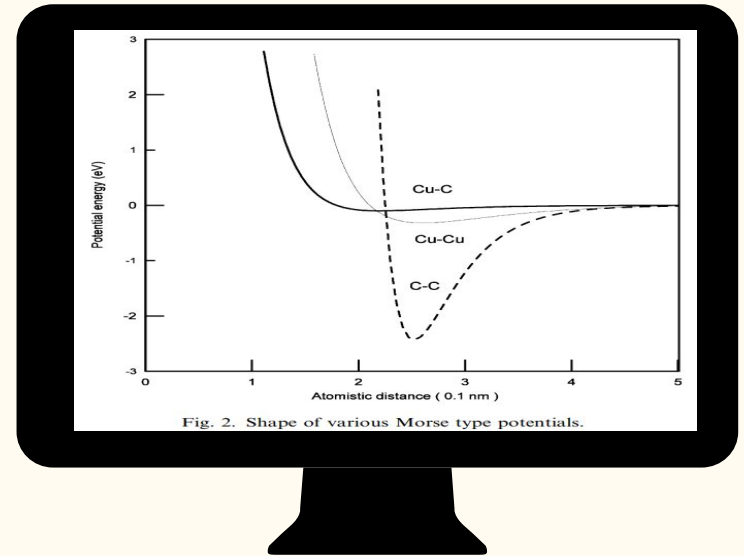
# Simulation Parameters

- Copper Sample and Diamond Pin tool used

- Indentation Speed was set to 100m/s

- Sixteen thousand atoms were used and arranged in 800 atoms per layer with 20 layers in depth

- Time Step was set to 1fs

- The atomic array model of the surface was constructed for a specific temperature at equilibrium and the velocities of atoms of the sample at this state are satisfied with a Maxwell distribution.

# OBSERVATIONS



(a-1) Initial condition
(b-1)

(a-2) Maximum indentation
(b-2)

(a-3) Residual dimple after indentation
(b-3)
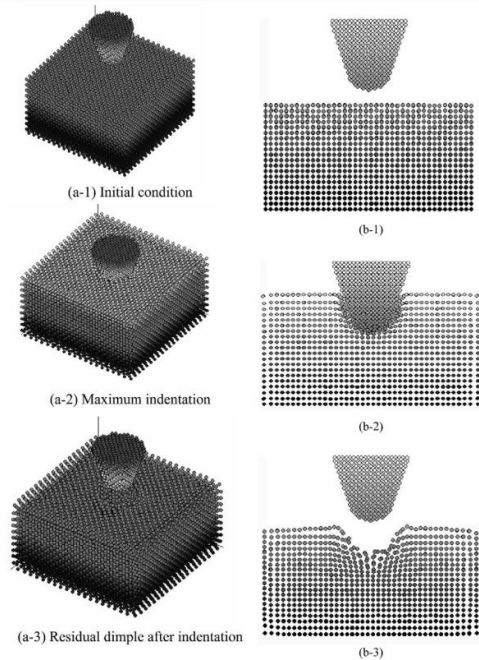
Fig. 3. (a) Positions at different stages of the nanoindention process. (b) Positions at different stages of the nanoindention process.

A residual dimple in the copper is observed after indentation by the diamond tool, as shown in Fig. 3(a-3).

The formation of this residual dimple is due to unrecoverable plastic deformation.

At maximum indentation depth (Fig. 3(a-3) and (b-3)), it is observed that the atomic order beneath the indenter differs considerably from its original pattern.
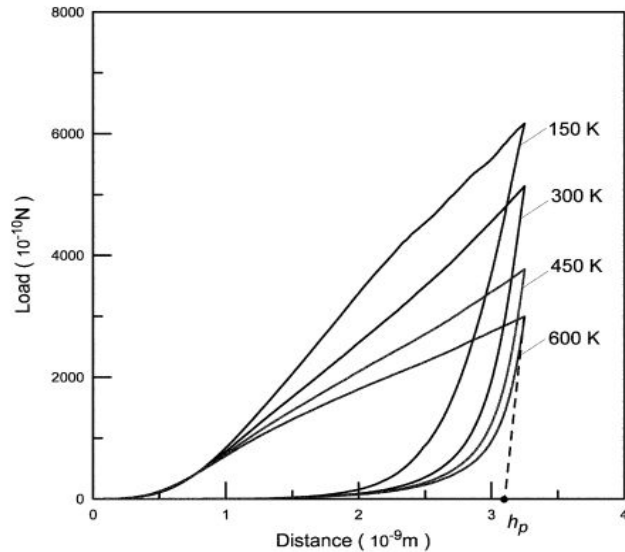
# OBSERVATIONS



Fig. 4. Load–distances of nanoindentation process varies at different temperatures.

Plastic indentation depth is seen to increase with increasing temperature.

Elastic recovery is smaller at a higher temperatures. The explanation of this phenomenon from the microscopic viewpoint is that the workpiece interatomic interaction forces, including repulsive and attractive forces, become weaker as the workpiece interatomic distance increases as a result of higher temperature.

# RESULTS AND CONCLUSIONS

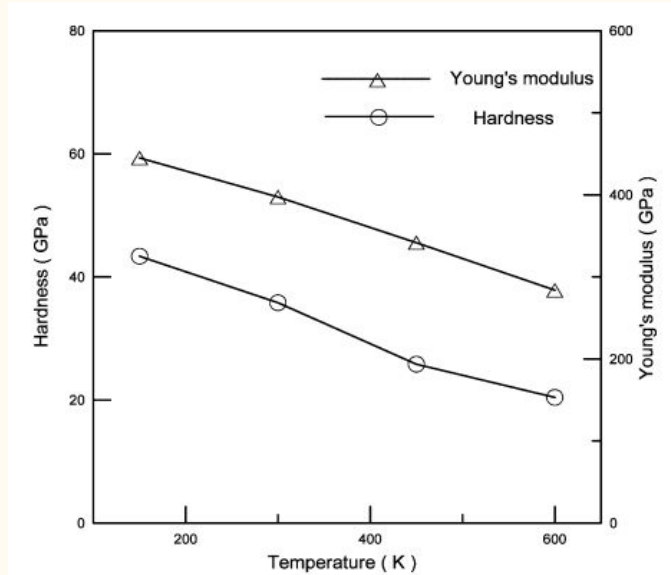## TEMPERATURE EFFECT ON THE TRIBOLOGICAL PROPERTIES



Fig. 6. Young's modulus and hardness at different temperatures.

**Result**:As temperature rises, Young's modulus and hardness both decline

This behaviour is consistent with the macro-behaviour

**Conclusion**:From a micro-scale perspective, the interatomic bonding energy of the workpiece reduces as the interatomic distance and temperature rise, which results in a reduction in hardness

# Other Applications of MD Simulation in Nanoindentation
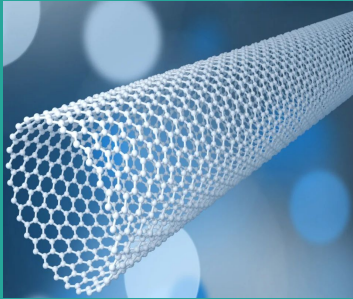


MD simulation of Nanoindentation has been used to investigate between tool tip and workpiece.These include

- Adhesion and Fracture of the Workpiece
- Nanoscale etching and indentation by a Carbon Nanotube
- Phase Transformations
- Elastic and Plastic Contact Behavior
- Influence of various tools on indentation mechanism

# References

https://core.ac.uk/download/pdf/237183758.pdf

https://doi.org/10.1016/S0921-5093(03)00219-3

https://www.ncbi.nlm.nih.gov/pmc/articles/PMC7558827/

# THANK YOU